Maciej PAŃCZYK
Jan SIKORA

A NEW IMAGING ALGORITHM FOR ELECTRIC CAPACITANCE TOMOGRAPHY

ABSTRACT *A new imaging algorithm of permittivity for Electrical Capacitance Tomography (ECT) was proposed in this paper. Some aspects of sensitivity analysis and the application of adjoint variables were discussed. In the final section of this paper some advantages and disadvantages were shown.*

Keywords: *Electric Capacitance Tomography, Partial Differential Equations, Adjoint Equation, Inverse Problem*
DOI: 10.5604/01.3001.0009.4405

1. INTRODUCTION

The motivation for writing this work is the need to build a hybrid tomograph, combining the possibility of electrical impedance tomography and electrical capacitance tomography. The main problem is designing compact electrodes suitable for both tomography types. Impedance Tomography is already a mature technology in the field of both imaging and hardware [6, 7, 8, 9, 14]. Measuring is more difficult in capacitance tomography [12, 15]. Colleagues from the Warsaw University of Technology, Faculty of Electronics and Information Technology are working on the latest generation of such a tomograph: the ETV4, with internationally unique operating parameters [2].

The key point of imaging in electrical capacitance tomography (ECT) is to measure the capacitance between electrodes in order to create a dielectric property distribution image. The aim of this study is to present an alternative imaging method

Maciej PAŃCZYK Ph.D. (Eng.)[1)]
e-mail: m.panczyk@pollub.pl

Jan SIKORA Ph.D., D.Sc. (Eng.)[1, 2)]
e-mail: sik59@wp.pl

[1)] Faculty of Electrical Engineering and Computer Science, Lublin University of Technology, Nadbystrzycka 38A, 20 618 Lublin,
[2)] Electrotechnical Institute, M. Pożaryskiego 28, 04-703 Warszawa

that does not require the measurement of capacitance, which is usually very small and difficult to measure [1, 2, 5]. The rule in Field Theory is that quantities which are difficult to measure are also extremely difficult to use in numerical calculations.

It should be emphasized that existing ECT applications are mainly associated with the imaging of multiphase flow in pipelines in the petrochemical industry, and with the control of the emptying of silos (see the work of Prof. D. Sankowski's team from the Institute of Applied Computer Science, or the work of R. Szabatin and W. Smolik's team from The Warsaw University of Technology, related to the 3D imaging of the dynamics of gas bubble release). The authors do not know of any work concerning the use of ECT for static objects, such as moisture in historical walls, for which other more or less invasive methods are prohibited by law. Such work is provided by the Lublin company NETRIX led by T. Rymarczyk. In cases like this, difficulties occur with the classical ECT algorithm because of the parasitic capacitances that occur due to an air layer which is difficult to determine ($\varepsilon_{r\_air} \approx 1.00054$), appearing between the electrode surface and the investigated object ($\varepsilon_{r\_brick} \approx 4.5$). This will act as a serial connection of three capacitors, with two small parasitic ones connected to the main one. Therefore it is necessary, just as in the medical application of ultrasound, to use coupling gel (of high permittivity) that minimizes the impact of parasitic capacitances.

The disadvantages of the classical ECT algorithm have inspired a search for new and better solutions. Another reason for our proposal is the concept for building a hybrid impedance-capacitance tomograph which is a research objective of the NETRIX company. Such a tomograph would simplify both the sensors, and capacitance sensor installation in closed metal ducts.

2. IMAGING ALGORITHMS FOR ELECTRICAL CAPACITANCE TOMOGRAPHY

The relationship between the capacity and distribution of electric permittivity can be formulated as follows [4]:

$$C = \frac{Q}{V} = -\frac{1}{V}\iint_{\Gamma} \varepsilon(x,y)\nabla\varphi(x,y)\,\mathrm{d}\Gamma\,, \tag{1}$$

where:

Q – is the electric charge accumulated at the electrode surface,

V – represents the potential difference between the electrodes whose capacitance is measured,

$\varepsilon(x,y)$ and $\phi(x,y)$ represent respectively the distribution of electric permittivity and electric potential,

Γ – represents the electrode surfaces.

The inverse problem is trying to estimate the permeability distribution on the basis of the measured capacity set. In practice the linearized mathematical model can be simplified to the relationship [1, 2]:

$$\boldsymbol{SG} = \boldsymbol{C} + \boldsymbol{r}, \tag{2}$$

where $\boldsymbol{G}$ is the $n\times1$ vector of standardized sought permeability; $\boldsymbol{C}$ represents the $m\times1$ vector of normalized capacity; $\boldsymbol{r}$ is the $m\times1$ vector representing the measurement noise; $\boldsymbol{S}$ is an $m\times n$ matrix, called the sensitivity matrix, which is determined by the relationship [3, 4, 5]:

$$S_{i,j}(x,y) = -\int_{p(x,y)} \frac{E_i(x,y)}{V_i}\frac{E_j(x,y)}{V_j}\mathrm{d}x\,\mathrm{d}y, \tag{3}$$

where $S_{i,j}(x,y)$ defines the sensitivity between the *i*-th and *j*-th electrode at a point (or pixel) $p(x,y)$; $E_i(x,y)$ is the distribution of the electric field intensity in the area where the *i*-th electrode is connected to the voltage source V_i.

Depending on the research centre, various measurement protocols are used and therefore different ways of selecting the *i* and *j* indexes. According to equation (2) the measurement and capacity calculations are the essence of the imaging algorithm. In field theory, there are three basic methods for determining the capacity [11].

3. THREE WAYS OF DETERMINING THE CAPACITY

3.1. Capacity determination using Gauss' law

The capacitance definition is:

$$C = \frac{Q}{U} \tag{4}$$

where Q is the electric charge on the surface of the electrode, and U is the voltage between the electrodes. The electric charge is calculated using Gauss' law:

$$Q = \oint_S \vec{D}\cdot\mathrm{d}\vec{s} \tag{5}$$

As a result we receive the following formula:

$$C = \left|\frac{1}{U}\int_\Gamma \varepsilon\frac{\partial\varphi}{\partial n}\mathrm{d}\Gamma\right| \tag{6}$$

At this point there is a problem: if the marginal effects are not taken into account an error of up to 9%, and more than 20% in 3D cases, can occur. [9, 13]. Please note that in ECT there are many electrodes located close to each other, therefore marginal effects play a significant role.

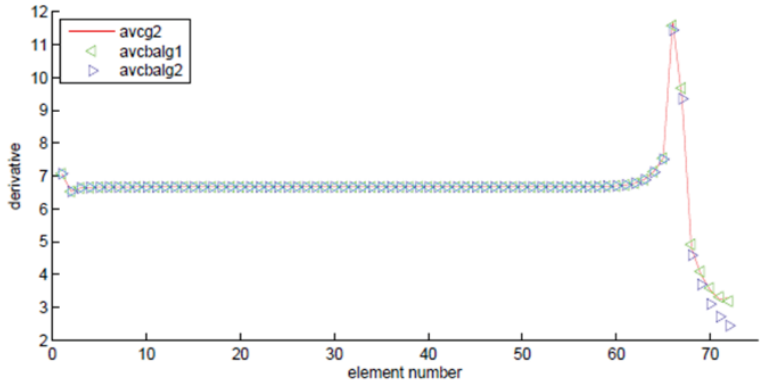

Fig. 1. Marginal effects on the electrode [13]

Despite this fact, this method is used in most imaging algorithms. Only in [3] was the method of determining the capacity on the basis of energy used. In the finite element method, which is commonly employed, the energy functional is minimized so capacitance can be much more accurately and easily determined compared to the electrostatic field intensity. The last quantity is determined by numerical differentiation, and this introduces significant calculation errors. It is important to bear in mind marginal effects, which, due to generally modest discretization, can be very influential, especially in 3D cases.

3.2. Capacity determination on the basis of the energy stored in an electrostatic field

The energy stored in the electrostatic field is calculated from the formula [3,11]:

$$W = \iiint_V \frac{\varepsilon E^2}{2}\,\mathrm{d}v = \frac{CU^2}{2} \tag{7}$$

Let us remember that, for example in FEM, the energy functional is minimized, so energy can be determined as a primary quantity and therefore much more accurately, as opposed to the previous method [10].

3.3. Capacity determination on the basis of the field image

The idea of this method is to treat the sufficiently small sub-areas defined by intersecting equipotential and field lines as flat capacitors. These small capacitors have a width Δy_{ij} and a distance between the capacitor plates Δx_{ij}.

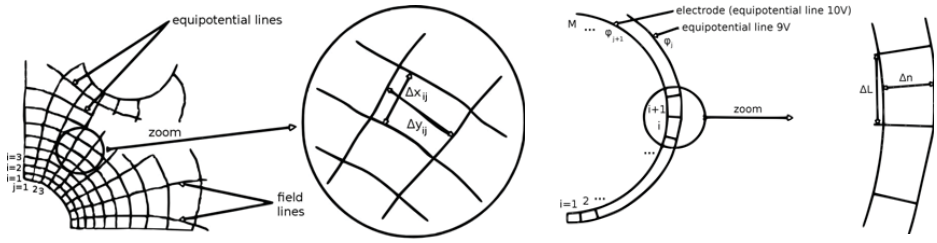

Fig. 2. Field image and an approximate method of determining capacity [11]

$$C_{ij} = \frac{\varepsilon_{ij} l \Delta y_{ij}}{\Delta x_{ij}} \tag{8}$$

The capacity of a single layer (between the equipotential lines, see Fig. 2) is the sum of the capacity of the cells lying in that layer (parallel capacitor connection).

$$C_j = \sum_{i=1}^{M} \frac{\varepsilon_{ij} l \Delta y_{ij}}{\Delta x_{ij}} \tag{9}$$

where M is the number of cells lying in the layer.

The total capacity is equal to the inverse of the sum of the inverse of the capacitance layer (serial connection).

$$C = 1 / \sum_{i=1}^{N} 1 / C_j \tag{10}$$

where N – number of layers.

3.4. The choice of the method for determining capacity

The third way is not very practical because it does not offer the possibility to create an automatic algorithm, and therefore it is not taken into account. So, we have to choose one of the other two methods. Which one should we choose? Which method is more accurate, and less demanding of computing resources?

As far as accuracy is concerned, based on the laboratory tests presented in [11], the level of error in the energy method can be estimated to reach 1.5%. However, the definitional method, where the error may reach 9%, is even less accurate, due to the marginal effects or discretization.

Of course, these rates of error are approximate depending on the problem. Also, as already mentioned, the energy is a primary quantity and does not require additional transformations. Despite this, many authors unfortunately choose a definitional method!

4. ELECTRICAL IMPEDANCE TOMOGRAPHY AND ELECTRICAL CAPACITANCE TOMOGRAPHY – – MATHEMATICAL SIMILARITIES

4.1. Forward problem

Electrical properties such as conductivity σ [S/m] and electrical permittivity ε [F/m] define the behaviour of a material under the influence of an external electric field. For example, conductive materials have high conductivity σ for both DC and AC. Dielectric materials have a high permittivity, allowing only alternating current. Consider a complex function of conductivity:

$$\gamma(\boldsymbol{x},\omega) = \sigma(\boldsymbol{x}) + \mathrm{i}\omega\varepsilon(\boldsymbol{x}), \qquad \mathrm{i} = \sqrt{-1}\,, \tag{11}$$

where $\boldsymbol{x}$ is a positional vector in a 2D space depending on coordinates x, y, and ω is the pulsation.

A forward problem solution involves solving the Laplace equation for the EIT:

$$\mathrm{div}(\gamma\,\mathrm{grad}\varphi) = 0\,, \tag{12}$$

with Dirichlet boundary conditions on the attachment points of the current electrodes and Neumann boundary conditions on the rest of the boundary.

If $\omega = 0$, then we are dealing with resistive tomography, and when the imaginary part of complex conductivity is much larger than its real part (resistivity) and is capacitive, then the electrical impedance tomography acts as capacitive tomography.

In practice three terms are used: impedance tomography which refers to resistive tomography, capacitive tomography and induction, or eddy current, tomography, also called magnetic tomography by some authors. All three kinds of tomography are included in the group of impedance tomography, just having different characters: resistive, capacitive or inductive.

In the rest of the article we will use the algorithm suitable for impedance tomography (resistive tomography), therefore to simplify the text we can introduce a material factor $k(x, y)$, which will represent resistivity (or in practice conductivity) and in other cases it will represent the permittivity ε.

The solution of the Laplace equation is equivalent to finding the minimum of the functional of form [10]:

$$F(\varphi) = \frac{1}{2}\int_{\Omega} k(x,y)\left|\mathrm{grad}\varphi\right|^2 \mathrm{d}\Omega\,, \tag{13}$$

where $k(x, y)$ represents a material factor γ or ε.

This is to determine the minimum of the functional of the variable φ. Using the finite element method this means calculating nodal values corresponding to the stationary point $F(\varphi)$. This point is reached when the nodal values of φ satisfy the relation:

$$\frac{\partial F}{\partial \varphi} = \sum_{e=1}^{Me} \frac{\partial F^{(e)}}{\partial \varphi_i} = 0, \tag{14}$$

where *Me* is the number of finite elements, $i = 1, 2, ..., M$, and M is the number of nodes in the area.

After constructing the matrices that correspond to the equations of the individual finite elements, a system of M equations with M nodal values is created. In the analyzed area, there are $q = 2$ nodes, where the potential is described by the Dirichlet boundary conditions. Eliminating from the system of equations the variables which describe nodal potentials and satisfy the Dirichlet boundary conditions, the system of M-2 equations and M-2 variables φ gives the following formula [7, 9, 13]:

$$\boldsymbol{Y\varphi} = \boldsymbol{b} \tag{15}$$

This set of equations is called the equation of state. It should also be emphasized that for each position of the current electrodes $j = 1, 2, ..., p$, the equation of state has a different form.

4.2. Sensitivity analysis

The objective function is defined as the root mean square error value of the image construction [9]:

$$\Phi = \sum_{j=1}^{p} \Phi_j = 0.5 \sum_{j=1}^{p} \left(\boldsymbol{f}_j - \boldsymbol{v}_{0j} \right)^T \left(\boldsymbol{f}_j - \boldsymbol{v}_{0j} \right) = 0.5 \left(\left[\boldsymbol{F} \right] - \left[\boldsymbol{V}_0 \right] \right)^T \left(\left[\boldsymbol{F} \right] - \left[\boldsymbol{V}_0 \right] \right) \tag{16}$$

where:

$\boldsymbol{v}_{0j}$ – the measured voltage vector for the j-th position (j=1, 2, …, p) of the power source of n_{de} degrees of freedom,

$\boldsymbol{f}_j$ – the calculated voltage vector (based on the density distribution obtained in the current iteration step) for the j-th position of the power source,

Φ_j – the objective function for the j-th position of the power source,

Φ – the total objective function calculated for all positions,

$\left[\boldsymbol{V}_0 \right] = \left[\boldsymbol{v}_{01}, \boldsymbol{v}_{02}, ..., \boldsymbol{v}_{0p} \right]^T$,

$\left[\boldsymbol{F} \right] = \left[\boldsymbol{f}_1, \boldsymbol{f}_2, \ \ldots \ , \boldsymbol{f}_p \right]^T$.

The value of the objective function, for the established set of measurement data, depends on the matrix [$\boldsymbol{F}$], which is determined by analyzing a forward problem. [$\boldsymbol{F}$] is not only a function of the vector $\boldsymbol{\gamma}$, but also a function of the position of the power sources.

The gradient of the scalar objective function in relation to elements of the decision variable vector $\boldsymbol{\gamma}$ is given by the following formula:

$$\frac{\partial \boldsymbol{\Phi}}{\partial \boldsymbol{\gamma}} = \frac{\partial}{\partial \boldsymbol{\gamma}} \sum_{j=1}^{p} \boldsymbol{\Phi}_j = \sum_{j=1}^{p} \frac{\partial \boldsymbol{\Phi}_j}{\partial \boldsymbol{\gamma}}, \tag{17}$$

and

$$\frac{\partial \boldsymbol{\Phi}_j}{\partial \boldsymbol{\gamma}} = \left[\frac{\partial \boldsymbol{\Phi}_j}{\partial \gamma_1}, \frac{\partial \boldsymbol{\Phi}_j}{\partial \gamma_2}, ..., \frac{\partial \boldsymbol{\Phi}_j}{\partial \gamma_n} \right]^T. \tag{18}$$

The objective function is an implicit function of the decision variable vector $\boldsymbol{\gamma}$.

$$\boldsymbol{\gamma} = \left[\gamma_1, \gamma_2, ..., \gamma_n \right]^T. \tag{19}$$

The gradient of the objective function with respect to the vector $\boldsymbol{\gamma}$ has the form:

$$\left[\frac{\partial \boldsymbol{\Phi}_j}{\partial \gamma} \right] = \left[\frac{\partial \boldsymbol{\Phi}_j}{\partial \varphi_j} \right] \left[\frac{\partial \varphi_j}{\partial \gamma} \right], \tag{20}$$

where:

$$\left[\frac{\partial \boldsymbol{\Phi}_j}{\partial \left[\varphi_j \right]^T} \right] = \left[\frac{\partial \boldsymbol{\Phi}_j}{\partial \varphi_{j1}}, \frac{\partial \boldsymbol{\Phi}_j}{\partial \varphi_{j2}}, \ ..., \frac{\partial \boldsymbol{\Phi}_j}{\partial \varphi_{j(M-q)}} \right], \tag{21}$$

and:

$$\left[\varphi_j \right] = \left[\varphi_{j1}, \varphi_{j2}, \ ... \ , \varphi_{jn} \right]^T. \tag{22}$$

$$\left[\frac{\partial \left[\varphi_j \right]}{\partial \left[\gamma \right]} \right] = \begin{bmatrix} \frac{\partial \varphi_{j1}}{\partial \gamma_1} & \frac{\partial \varphi_{j1}}{\partial \gamma_2} & \cdots & \frac{\partial \varphi_{j1}}{\partial \gamma_{(M-q)}} \\ \frac{\partial \varphi_{j2}}{\partial \gamma_1} & \frac{\partial \varphi_{j2}}{\partial \gamma_2} & \cdots & \frac{\partial \varphi_{j2}}{\partial \gamma_{(M-q)}} \\ \vdots & \vdots & \ddots & \vdots \\ \frac{\partial \varphi_{j(M-q)}}{\partial \gamma_1} & \frac{\partial \varphi_{j(M-q)}}{\partial \gamma_2} & \cdots & \frac{\partial \varphi_{j(M-q)}}{\partial \gamma_{(M-q)}} \end{bmatrix}. \tag{23}$$

The basic problem in determining the vector $\left[\frac{\partial \boldsymbol{\Phi}_j}{\partial \boldsymbol{\gamma}}\right]$ is to determine the term $\left[\frac{\partial \boldsymbol{\varphi}_j}{\partial \boldsymbol{\gamma}}\right]$ described by formula (23). These derivatives can be obtained by testing the absolute sensitivity of the equation of state for the individual decision variables [9].

To do this, it is necessary to make a differentiation on both sites of the equation of state $\boldsymbol{Y}\boldsymbol{\varphi} = \boldsymbol{b}$ for the *j*-th position of the current electrodes in terms of material factors $\boldsymbol{\gamma}$:

$$\left[\boldsymbol{Y}_j\right]\left[\frac{\partial \boldsymbol{\varphi}_j}{\partial \boldsymbol{\gamma}}\right] + \frac{\partial}{\partial \boldsymbol{\gamma}}\left(\left[\boldsymbol{Y}_j\right]\left[\tilde{\boldsymbol{\varphi}}_j\right]\right) = \left[\frac{\partial \boldsymbol{b}_j}{\partial \boldsymbol{\gamma}}\right], \tag{24}$$

where $\tilde{\boldsymbol{\varphi}}_j$ is the state vector of the previous iteration, the components of which are treated as constant expressions in the partial derivative.

The matrix $\left[\boldsymbol{Y}_j\right]$ is non-singular, so you can make the transformation:

$$\left[\boldsymbol{Y}_j\right]\left[\frac{\partial \boldsymbol{\varphi}_j}{\partial \boldsymbol{\gamma}}\right] = \left[\frac{\partial \boldsymbol{b}_j}{\partial \boldsymbol{\gamma}}\right] - \frac{\partial}{\partial \boldsymbol{\gamma}}\left(\left[\boldsymbol{Y}_j\right]\left[\tilde{\boldsymbol{\varphi}}_j\right]\right), \tag{25}$$

$$\left[\frac{\partial \boldsymbol{\varphi}_j}{\partial \boldsymbol{\gamma}}\right] = \left[\boldsymbol{Y}_j\right]^{-1}\left(\left[\frac{\partial \boldsymbol{b}_j}{\partial \boldsymbol{\gamma}}\right] - \frac{\partial}{\partial \boldsymbol{\gamma}}\left(\left[\boldsymbol{Y}_j\right]\left[\tilde{\boldsymbol{\varphi}}_j\right]\right)\right), \tag{26}$$

After the substitution of (26) to (20), the following equation is received:

$$\left[\frac{\partial \boldsymbol{\Phi}_j}{\partial \boldsymbol{\gamma}}\right] = \left[\frac{\partial \boldsymbol{\Phi}_j}{\partial \tilde{\boldsymbol{\varphi}}_j}\right]\left[\boldsymbol{Y}_j\right]^{-1}\left(\left[\frac{\partial \boldsymbol{b}_j}{\partial \boldsymbol{\gamma}}\right] - \frac{\partial}{\partial \boldsymbol{\gamma}}\left(\left[\boldsymbol{Y}_j\right]\left[\tilde{\boldsymbol{\varphi}}_j\right]\right)\right). \tag{27}$$

Denoting by $\boldsymbol{\lambda}_j$:

$$\boldsymbol{\lambda}_j = \left[\left[\frac{\partial \boldsymbol{\Phi}_j}{\partial \boldsymbol{\varphi}_j}\right]\left[\boldsymbol{Y}_j\right]^{-1}\right]^T = \left[\left[\boldsymbol{Y}_j\right]^{-1}\right]^T\left[\frac{\partial \boldsymbol{\Phi}_j}{\partial \boldsymbol{\varphi}_j}\right]^T = \left[\boldsymbol{Y}_j\right]^{-1}\left[\frac{\partial \boldsymbol{\Phi}_j}{\partial \boldsymbol{j}_j}\right]^T. \tag{28}$$

Left multiplying the above relation by $\left[\boldsymbol{Y}_j\right]$ we receive:

$$\left[\boldsymbol{Y}_j\right]\boldsymbol{\lambda}_j = \left[\boldsymbol{Y}_j\right]\left[\boldsymbol{Y}_j\right]^{-1}\left[\frac{\partial \boldsymbol{\Phi}_j}{\partial \boldsymbol{\varphi}_j}\right]^T. \tag{29}$$

This is the adjoint equation to the equation of state (12), and $\boldsymbol{\lambda}_j$ is the adjoint vector to the state vector for the *j*-th position of the electrodes $\boldsymbol{\varphi}_j$.

The adjoint variable $\boldsymbol{\lambda}$ method involves solving the adjoint equation in relation to the adjoint vector and using this vector to compute the gradient of the objective function with respect to elements of the decision variable vector.

The construction of the adjoint does not require too many numerical operations. The left side of this equation is the same as the equation of state, therefore the designation of the adjoint vector, reduced state matrix $\boldsymbol{Y}_j$ from equation (15), is used, which is determined by solving the forward problem.

4.3. Calculation of the first expression member for the gradient of the objective function

In order to determine the right side of the adjoint equation (3.49) it is necessary to differentiate the objective function for the *j*-th position of the power supply relative to the nodal potential vector $\boldsymbol{\varphi}_j$:

$$\left[\frac{\partial \boldsymbol{\Phi}}{\partial \boldsymbol{\varphi}_j}\right] = 0.5\left(\sum_{i=1}^{n_{de}}\left(f_{ji} - \nu_{0\,ji}\right)^2\right). \tag{30}$$

Assuming that the electrodes are indicated by sequential natural numbers k = 1,2, ..., -2, (from the first voltage electrode, next to the current electrode attached to a voltage source, in a clockwise direction), the derivative of the objective function with respect to the potential of the *l*-th node belonging to the electrode number k is:

$$\frac{\partial \Phi}{\partial \varphi_{jl}} = \begin{cases} f_{jk} - \nu_{0\,jk}, & \text{for } k = 1; \\ f_{jk} - \nu_{0\,jk} - \left(f_{jk-1} - \nu_{0\,jk-1}\right), & \text{for } k = 2,...,13; \\ -\left(f_{jk-1} - \nu_{0\,jk-1}\right), & \text{for } k = 14; \end{cases} \tag{31}$$

where:

$\frac{\partial \Phi_j}{\partial \varphi_{jl}}$ – *l*-th element of vector $\left[\frac{\partial \Phi_j}{\partial \varphi_j}\right]$,

f_{jk} – *k*-th element of vector $\boldsymbol{f}_j$,

$\nu_{0\,jk}$ – *k*-th element of vector $\boldsymbol{\nu}_{0j}$.

For all other nodes (which are not connected to the voltage electrodes) $\frac{\partial \Phi_j}{\partial \varphi_{jl}} = 0$.

4.4. Physical interpretation of the adjoint variable λ

By analogy with the equations of state we can conclude that the adjoint equation is created by an approximation of the Poisson equation with respect to adjoint variable λ, using the finite element method:

$$\text{div}\,(k\,\text{grad}\,\lambda) = -\mu. \tag{32}$$

The function μ of the source in equation (32) is different from zero only in the nodes of the heterogeneous Dirichlet boundary condition type. In the other part of the right side of the adjoint equation it is equal to zero.

On this basis one can conclude that the value of the function of the source of the adjoint equation represents the mismatch between the values of the measured potentials and the appropriate potentials calculated in this iteration of the optimization. In the final stage of calculating, the value of the function of the source μ should approach zero. This occurs when the electrical conductivity calculated in the designated iteration step corresponds to the real distribution of electrical conductivity in the analyzed object.

In the case of impedance tomography the source of the adjoint variable is located on the edge of the area, therefore the method for adjoint variable sensitivity analysis can be called the boundary method. This will require precise approximation of the edge of the area.

The distribution of the adjoint variable for four successive power source positions (where the powered electrodes are adjacent) is shown in Figure 3.

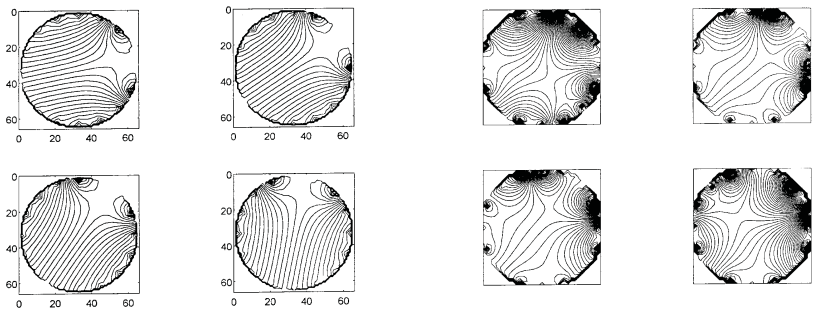

Fig. 3. Adjoint variable images in two cases, for the approximation of polygonal chain lines (left) and the stepped line (right)

For imaging purposes, it is best to use elements of a shape corresponding to the pixel elements i.e. square ones, where dielectric permittivity is changing inside the element interior [10]. This approach to area discretization has many advantages including:

- the ability to map any shape without additional effort (although the edges will be described by a stepped function),
- significant acceleration of the forward problem solution by use of identical elements for the discretization,
- relatively easy isoparametric square element symbolic integration.

Unfortunately, there are also some disadvantages of this type of discretization – the stepped approximation of the edge area increases errors in solving the adjoint state. This has a significant impact on the determination of the direction of improvement. Figure 3 shows equipotential lines for the adjoint variable λ for the first four positions of the energy source in the case of an approximation made using polygonal chain lines. When the lines are smooth, symmetry is maintained relative to the supply system and the surface representing the distribution of λ is smooth (see Fig. 4).

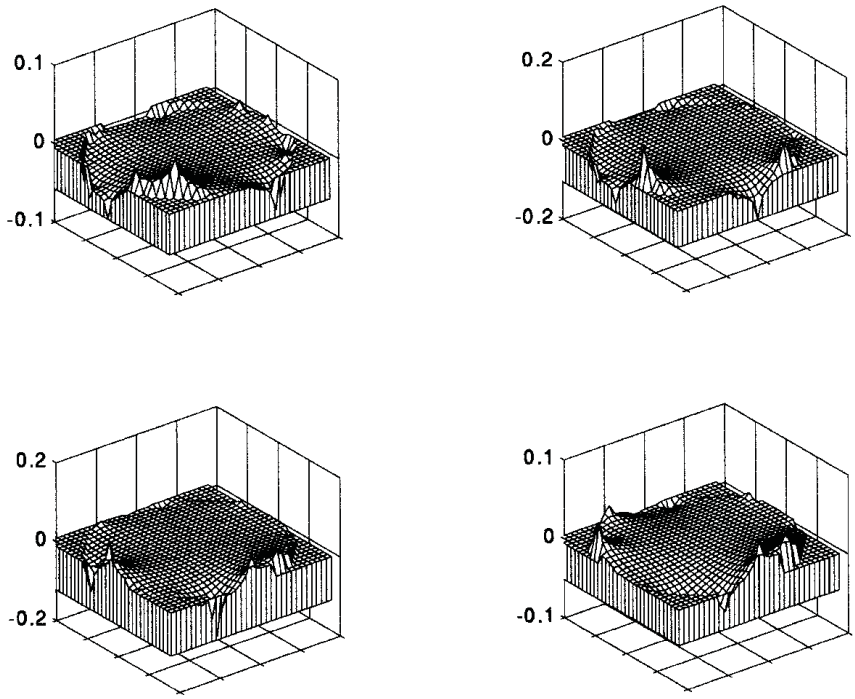

Fig. 4. The surface representing the distribution of the adjoint variable for the first four positions of the current power source, in the case of an approximation by polygonal chain lines

If, for discretization, a square element is used, the edge of the area is approximated by a stepped line. This has a significant impact on the behaviour of the equipotential line adjoint variable λ (Fig. 3).

The problems associated with the approximation of the edge may be largely mitigated by increasing the discretization (a stepped curve will then adhere better to the contours of the analyzed area). However this increases the number of decision variables and, therefore, makes the calculation time longer. Such an approach only alleviates the problem but does not solve it completely.

5. CONCLUSIONS

The article presents a new approach to the imaging algorithm in Electrical Capacitance Tomography. Motivation for this was provided by the work on hybrid tomography at the Netrix company led by T. Rymarczyk [7, 8]. The advantages and disadvantages of the proposed method are presented in table 1.

TABLE 1
Advantages and disadvantages of the proposed imaging method

Advantages	Disadvantages
Simplified hybridization of electrical impedance tomography (EIT) and electrical capacitance tomography (ECT)	A slower imaging algorithm, at present not applicable to dynamic process imaging (in some applications, it is irrelevant – static images are sufficient)
The ability to integrate the measurement electrodes for the EIT and ECT	Sensitivity analysis required
Easier and probably faster acquisition of measured quantities	If during the sensitivity analysis a adjoint variable is used the boundary curves have to be precisely approximated.
Simpler electronic hardware	
Easier discretization with a smaller number of nodes due to the shape of the electrodes	
The possibility of applications in closed metal channels, excluding those for explosive medium transportation.	

LITERATURE

1. Chaniecki Z., Dyakowski T., Niedostatkiewicz M., Sankowski D.: “Application of Electrical Capacitance Tomography for Bulk Solids Flow Analysis in Silos”. Particle & Particle Systems Characterization., 2006, vol. 23, no. 3-4, pp. 306-312, ISSN: 0934-0866.
2. Czarnecki P., Smolik W., Szabatin R.: “Electrical Capacitance Tomography System Architecture”, w: Electrical Capacitance Tomography / Sankowski Dominik, Sikora Jan (red.), 2010, ISBN 978-83-61956-00-6, ss. 25.
3. Elmy Johana Mohamad, Muhammad AfiqZimam Mohamed, Ruzairi Abdul Rahim, Leow Pei Ling, Mohd. Hafiz Fazalul Rahiman, Khairul Hamimah Abas and Salinda Bunyamin: “Sensor modeling for portable electrical capacitance tomography system using simulation by COMSOL MULTIPHYSICS”, Int. Journ. Of Innovative Computing, Information and Control, vol. 8, no. 10(B), 2012, pp. 6999-7016.
4. Jing Lei, Shi Liu, Xueyao Wang, Qibin Liu: “An Image Reconstruction Algorithm for Electrical Capacitance Tomography Based on Robust Principle Component Analysis”, Sensors 2013, 13, 2076-2092, doi:10.3390/s130202076.

5. Kryszyn J., Smolik W., Olszewski T. et al: “Elektryczny tomograf pojemnościowy EVT4”, Elektronika - konstrukcje, technologie, zastosowania, SIGMA NOT, nr 7, 2015, ss. 12-15, DOI:10.15199/13/2015.7.2 (“Electrical capacitance tomograph EVT4” – in Polish).
6. Pańczyk, M., Sikora, J.: “Boundary element method application in wall dampness tomography”, Przegląd Elektrotechniczny, 03/2016, pp. 96-98.
7. Rymarczyk T.: “Systemy tomografii procesowej w bezinwazyjnych pomiarach diagnostycznych”, Inżynieria bezwykopowa, pp. 66-72, 1/2014 (“Systems for process tomography in non-invasive diagnostic measurements” – in Polish).
8. Rymarczyk T.: “Using electrical impedance tomography to monitor flood banks”, International Journal of Applied Electromagnetics and Mechanics, (45), pp. 489-494, 2014.
9. Sikora J.: “Numeryczne algorytmy w tomografii impedancyjnej i wiroprądowej”, Oficyna Wydawnicza Politechniki Warszawskiej, 2000 (“Numerical algorithms in impedance tomography and eddy current tomography” – in Polish).
10. Sikora J.: “Numeryczne metody rozwiązywania zagadnień brzegowych; Podstawy metody elementów skończonych i metody elementów brzegowych”, Wydawnictwo Politechniki Lubelskiej, Lublin 2009 (“Numerical methods for solving boundary value problems; Fundamentals of the finite element method and boundary element method” – in Polish).
11. Starzyński J.: “Laboratorium podstaw elektromagnetyzmu”, WPW, 2005 (“The Introductory Electromagnetism Laboratory” – in Polish).
12. Wajman R., Banasiak R., Mazurkiewicz Ł., Dyakowski T., Sankowski D.: “Spatial imaging with 3D capacitance measurements”. Measurement Science and Technology, vol. 17, no. , pp. 2113-2118, 2006, ISSN: 0957-0233 (“Open source, object-oriented library of the boundary element method to solve the diffusion tomography problems”, PhD thesis – in Polish).
13. Wieleba P.: Otwarta, obiektowa biblioteka metody elementów brzegowych do rozwiązywania zagadnień tomografii dyfuzyjnej, Praca doktorska, Instytut Elektrotechniki, Warszawa, 2010.
14. “Industrial and Biological Tomography: Theoretical Basis and Applications”, edited by J. Sikora and S. Wójtowicz, Wydawnictwo IEL, Warszawa 2010.
15. “Electrical Capacitance Tomography: Theoretical Basis and Applications”, edited by D. Sankowski and J. Sikora, Wydawnictwo IEL, Warszawa 2010.

Accepted for publication 14.10.2016

NOWY ALGORYTM OBRAZOWANIA W ELEKTRYCZNEJ TOMOGRAFII POJEMNOŚCIOWEJ

Maciej PAŃCZYK, Jan SIKORA

STRESZCZENIE *W pracy przedstawiono „nowy" algorytm obrazowania przenikalności elektrycznej w Elektrycznej Tomografii Pojemnościowej. Omówiono aspekty związane z analizą wrażliwościową i zmienna sprzężoną. Przedstawiono jej interpretację fizyczną. Wskazano na zalety i wady zaproponowanej metody obrazowania.*

Słowa kluczowe: *elektryczna tomografia pojemnościowa, równania różniczkowe cząstkowe, równanie sprzężone, zagadnienie odwrotne*

Maciej PAŃCZYK, PhD Eng. – graduated from the Faculty of Electrical Engineering, Lublin University of Technology. He worked in the Department of Fundamental Electrical Engineering, Lublin University of Technology, then in the Information Technology Department at BDK S.A Bank and since 2004 at the Institute of Computer Science, Lublin University of Technology. His work focuses on programming and the Boundary Element Method development and applications.

Prof. Jan SIKORA, Ph.D., D.Sc. Eng. – graduated from the Faculty of Electrical Engineering at the Warsaw University of Technology. Over more than 34 years of work at his alma mater he achieved all grades, titles and positions, including the position of full professor. Since 1998 he has also worked in the Electrotechnical Institute in Warsaw. Since 2008 he has worked at the Faculty of Electrical Engineering and Computer Science at the University of Lublin in the Department of Electronics, later transformed into the Institute of Electronics and Information Systems. From 2001-2004 he worked as a Senior Research Fellow at University College London in the Prof. S.R. Arridge Group of Optical Tomography. His research interests are focused on numerical methods for electromagnetic fields and their applications in diffusion tomography.